Fluorescence Recovery after Two-Photon Bleaching for the Study of Dye Diffusion in Polymer Systems

Edward Van Keuren*,† and Wolfgang Schrof‡

Department of Physics, Georgetown University, Washington, DC 20057, and BASF AG, Ludwigshafen, Germany

Received January 7, 2003; Revised Manuscript Received May 6, 2003

ABSTRACT: Fluorescence recovery after two-photon photobleaching (TP-FRAP) was used to characterize the diffusion in polymer thin films. Using a two-photon/confocal microscope, a region was bleached inside a fluorophore-doped poly(vinyl alcohol) film. An ellipsoidal form of this spot was observed, and a simple form was derived for the fluorescence recovery at the spot center, enabling the local fluorophore diffusion coefficient to be determined. A series of films with varying amounts of added plasticizer were measured to determine the relation between plasticizer content and diffusion coefficient. In a second set of films with inhomogeneous distribution of plasticizer, three-dimensional maps of the diffusion coefficient were measured using TP-FRAP followed by confocal imaging. From these maps and the calibration curves, three-dimensional maps of the local plasticizer concentration were determined.

Introduction

The measurement of diffusion processes in polymer films is important both directly for applications such as printing and indirectly as a measure of film morphology and composition.[1] Depending on the characteristic time scales for the diffusion, various techniques are useful for measuring the diffusion coefficient, D, in cases in which the diffusion is linear. For rapid diffusion coefficients (10^{-8}−10^{-5} cm^2/s), time correlation spectroscopy methods are effective (photon correlation spectroscopy (PCS),[2] fluorescence correlation spectroscopy (PCS),[3,4] Raman correlation spectroscopy (RCS)[5]), as are other methods such as capillary flow.[6] This range of D values corresponds to single molecules or submicron-sized particles in low-viscosity liquids, i.e., rapid diffusion. On the other end of the spectrum, slow diffusion processes such as those in solids, with values of D on the order of 10^{-12}−10^{-8} cm^2/s, may be followed using methods such as NMR imaging[7] or optical methods such as interferometry or holographic relaxation spectroscopy (HRS).[8]

Another such method is fluorescence recovery after photobleaching (FRAP).[9−11] In this technique, fluorescent dye molecules in a limited region of a sample are irreversibly photobleached by high-power irradiation. The high-power light causes multiple excitations of the molecules, with correspondingly large probability that they will undergo an irreversible chemical reaction while they are in the less-stable excited state. Diffusion or other transport of unbleached dye molecules back into this region can be monitored in a number of ways, including total fluorescence emission[9−12] or fluorescence imaging.[13] By observing the recovery of the fluorescence signal with time and making certain assumptions about the geometry of the bleached region, the diffusion coefficient can be determined. The ability to control the time scales of the measurement by varying the size of the bleached region makes this a useful technique for relatively slowly diffusing species.[14]

The FRAP technique has been used by a number of groups to look at spatial variation in diffusion, either by pattern[15] or spot[16] photobleaching. A variation of this method is to use confocal optics to bleach a small region of a sample and subsequently image it.[17−19] In principle, this enables three-dimensional mapping of diffusion coefficients in materials. However, the bleach profile is linearly proportional to the local irradiance of the excitation beam. In confocal optics, this is simply the focused Gaussian beam shape or a double cone. The analysis of the recovery of the fluorescence into this bleached region in terms of diffusion is difficult.[21]

An alternative, which enables genuine three-dimensional resolution, is to use two-photon excitation to create bleach spots. Two-photon excitation is based on near-simultaneous absorption of two photons by a molecule and its subsequent fluorescence decay. The probability of two-photon excitation (and bleaching) depends on the square of the irradiance of the incident light. For a focused infrared beam, the irradiance is large enough to cause significant photoexcitation and bleaching only in the region near the focus, and ellipsoidal bleaching profiles have been measured.[22] Furthermore, it often has an advantage in terms of the depth of images that can be obtained, since the excitation light is in the near-infrared wavelength region, where there are typically fewer strong absorption bands in most materials, and scattering is also generally less.[23]

Two-photon excitation has been used in combination with nonimaging[24] and imaging[21,25,26] FRAP. This method has the advantage of providing real three-dimensional spatial information, since clearly defined spots are formed as opposed to extended double-cone structures. Here we demonstrate two-photon bleaching followed by confocal imaging to measure recovery of fluorescence in the bleached area of a polymer film. We demonstrate the ability to map out profiles of the diffusion coefficient in three dimensions and use this to study a composition gradient in a polymer film.

Experimental Procedure

Two-photon bleaching was done using the output of an Ar ion laser (Innova 200, Coherent, Inc.) pumped Ti:sapphire laser

† Georgetown University.
‡ BASF AG.
* Corresponding author: Tel +1-202-687-5982; e-mail vankeu@physics.georgetown.edu.

10.1021/ma034022s CCC: $25.00
Published on Web 06/06/2003

(Mira 900F, Coherent). The output pulses from the Mira were coupled into a combination two-photon/confocal microscope (DM IRBE inverted microscope, TCS SP confocal scanning head, Leica Microsystems, GmbH) through an optical fiber. To compensate for pulse dispersion in the fiber, the pulses passed through a fiber dispersion compensator (Coherent GDC) prior to entering the fiber, resulting in output pulses to the microscope being Fourier transform limited, with pulse widths of approximately 150 fs. The power level at the sample was typically around 30 mW. The experiments presented here were obtained using a 63×, 1.25 NA HCPL Fluotar oil immersion objective.

The bleaching was done at the maximum laser power for 10 ms, the minimum open time for the mechanical shutter that controlled the laser input to the sample. This bleach was rapidly repeated between 10 and 20 times to obtain a cleanly bleached spot. This tended to increase the size of the spot above the diffraction-limited value for this objective. Several pulses at shorter bleach times rather than a single long pulse were used to avoid thermal damage to the sample. Imaging was done with the confocal scanning head, with excitation from either an Ar ion laser ($\lambda = 488$ nm) or a Kr ion laser ($\lambda = 568$ nm). Imaging in the plane of the film is accomplished by the alignment mirror rastering across the field of view, while sections along the normal to the film are measured by movement of the stage. Imaging started immediately after the bleach step was complete and repeated at regular intervals after this in order to measure the recovery of fluorescence in the spot. We found that the delay between the final bleach pulse and the start of the imaging could have a significant effect on the results, especially for more rapid diffusion. Therefore, this delay was carefully measured and included in the analysis described below.

The results described below are on samples of PVA (poly(vinyl alcohol), MOWIOL 30/92 Clariant) doped with Rhodamine B, at concentrations of less than 0.1 wt %. The low concentrations prevented the dye from acting as a plasticizer for the polymer as well as avoiding significant aggregation of the dyes and reabsorption of the fluorescence emissions. Rhodamine B has a strong two-photon-allowed state around 3.0 eV for incident light at wavelength 840 nm[27,28] and has been used as a probe in two-photon pattern bleaching for studying structural deformations in polymers.[29] The polymer was first dissolved in deionized water, the dye added to the polymer solution, and films prepared by doctor blading (knife edge coating). Final film thicknesses were on the order of 30−50 μm.

Theory

The concentration profile after two-photon bleaching was been assumed to have a Gaussian profile in three dimensions, with the radius in the x and y directions equal. This assumption was justified by confocal 3D scans performed on a photobleached Rhodamine B doped PVA film. A cross section of a typical two-photon bleached spot is shown in Figure 1. Figure 2 shows the profiles through the bleached spot along the x and z axes. For the scan along the z axis, the pixel intensity in a small region of interest ($\sim 10^{-3}$ μm^2) at the bleach spot center was averaged in each cross section, and the results were plotted vs the confocal depth. The plot along the x-axis is of pixel intensity across the spot in the image at the focal plane. The averaging in the scan along the z-axis results in lower statistical variation between points. The relative statistical fluctuation in pixel intensities is on the order of 15%.

The form of the concentration profile as a function of radial coordinate ρ ($= \sqrt{x^2+y^2}$) and position z along the beam, and at time $t = 0$, is assumed to be

$$C(\rho,z) = C_0 - C_1 e^{-\rho^2/\rho_0^2} e^{-z^2/z_0^2} \qquad (1)$$

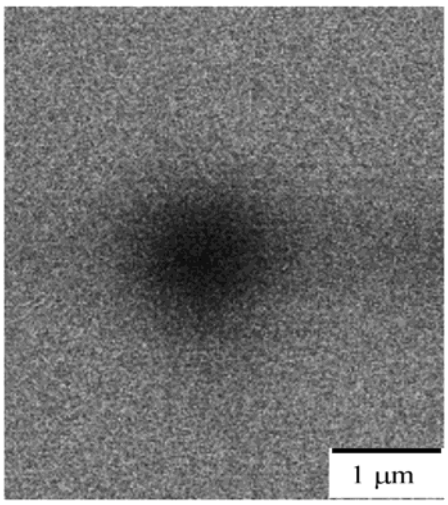

Figure 1. A typical bleached spot in a Rhodamine B doped PVA film.

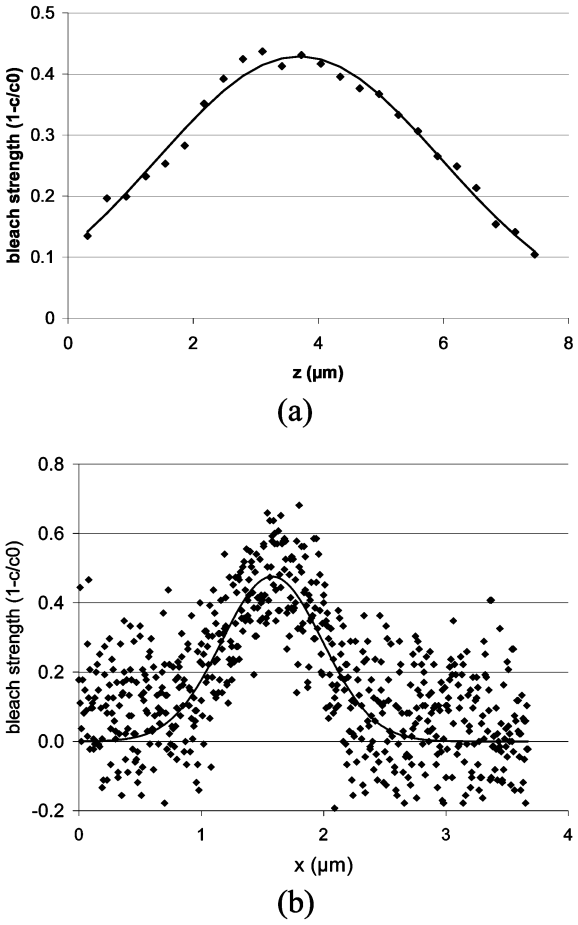

Figure 2. Spot bleach profiles along the (a) z axis and (b) x axis.

Here, C_0 is the concentration far from the bleached point, and $C_0 - C_1$ is the concentration of unbleached dye at the origin at time $t = 0$ and ρ_0 and z_0 are the 1/e radii of the spot. This function was fit to the spot bleached into the PVA/Rhodamine B films. The fitted curves are also shown in Figure 2. The average values of ρ_0 and z_0 were 0.52 μm and 3.3 μm, respectively. These values of the spot size were used in the data analysis.

We derived an analytic form for the fluorescence recovery at the spot center. The Green's function for the diffusion equation is[30]

$$C(r,t) \propto \frac{e^{-r^2/4Dt}}{(4Dt)^{3/2}} \tag{2}$$

This would be the concentration at a point **r** away from the origin at time *t*, if the source were a delta function concentration at the origin at time $t = 0$. Conversely, we can shift this source to a point **r** and have an identical equation for the concentration at the origin due to this point source.

We restrict our consideration to the concentration at the origin as a function of time. As we will show, this leads to a simple analytical form for the fluorescence recovery. The corresponding restriction on the experimental procedure is that the analysis was done for a small region in the center of the bleach profile. The ability to create three-dimensional images with confocal or two-photon imaging makes this procedure straightforward.

If we wish to calculate the concentration at the origin due to a distribution of sources in space, we need to integrate this function over that distribution, i.e.

$$C(\vec{r},t) \propto \int dV \frac{e^{-r^2/4Dt}}{(4Dt)^{3/2}} C(\vec{r},0) \tag{3}$$

where the concentration is not necessarily symmetric, so the position variable has been replaced by a vector. Inserting the concentration determined above, integrating over cylindrical coordinates, and using $r^2 = \rho^2 + z^2$ gives

$$C(\vec{r},t) \propto \int_{-\infty}^{\infty} dz \int_0^{\infty} \rho \, d\rho \frac{1}{(4Dt)^{3/2}} e^{-\rho^2/4Dt} e^{-z^2/4Dt} [C_0 - C_1 e^{-\rho^2/\rho_0^2} e^{-z^2/z_0^2}] \tag{4}$$

The integrals over ρ and z can be done separately, giving

$$C(\vec{r},t) \propto \frac{1}{(4Dt)^{3/2}} \left[C_0 (4Dt)^{3/2} - C_1 \left(\frac{1}{4Dt} + \frac{1}{\rho_0^2} \right)^{-1} \left(\frac{1}{4Dt} + \frac{1}{z_0^2} \right)^{-1/2} \right] = \left[C_0 - C_1 \left(1 + \frac{4Dt}{\rho_0^2} \right)^{-1} \left(1 + \frac{4Dt}{z_0^2} \right)^{-1/2} \right] \propto 1 - C' \left(1 + \frac{4Dt}{\rho_0^2} \right)^{-1} \left(1 + \frac{4Dt}{z_0^2} \right)^{-1/2} \tag{5}$$

Data were analyzed by first defining small regions of interest (ROI) near the center of the spot and in the background (unbleached) area of the image. The average of the central region pixel intensity was normalized with respect to that of the background intensity. These values as a function of time after bleaching were the data set that were fitted with the equation

$$1 - C \left(1 + \frac{4Dt}{\rho_0^2} \right)^{-1} \left(1 + \frac{4Dt}{z_0^2} \right)^{-1/2} \tag{6}$$

with the values of ρ_0 and z_0 measured separately. This yielded the diffusion coefficient D as the single fit parameter. We note here the implicit assumption in this derivation that the transport of molecules into the bleached region of the polymer was simple linear diffusion.

This analysis of the fluorescence recovery at the bleach spot center only allows the simple analytic form of eq 6 to be obtained. The total (integrated) fluorescence recovery in a two-photon bleached spot, as derived in ref 21, is a more complex infinite sum. In particular, a simple nonlinear curve fitting of eq 6 may be applied to the fluorescence intensity at the spot center with only two free parameters: the initial bleaching strength C and the diffusion coefficient D.

Results and Discussion

Effect of a Glycerin Softener on Dye Diffusion in Poly(vinyl alcohol). We measured a series of polymer films with varying concentration of an added softener. Glycerin is a good plasticizer for water-soluble polymers such as PVA.[31] We prepared films of PVA/glycerin by dissolving both in water and then doctor blading (knife edge coating) the mixtures. Figure 3 shows a typical time series of the recovery of the fluorescence for four spots bleached in a glycerin/PVA film. In the particular film shown in the figure, the glycerin concentration in PVA was approximately 33 wt %. Reversible photobleaching was not observed in the pure dye-doped polymer films (without glycerin), suggesting that the recovery in Figure 3 is due to translation diffusion of the dye back into the bleached region. Rotational diffusion may also be present from dyes that are unbleached because their molecular axes are perpendicular to the (optical) electric field of the beam. However, we would expect a relatively small percentage of the dye molecules inside the spot to remain unbleached because of this, and the time scale for fluorescence recovery from their rotational diffusion is likely to be much more rapid than that of the translation. Typical data (normalized to 1 at long times) and fits obtained from these images are shown in Figure 4.

The normalized data were fitted using eq 6, with the bleach strength C and the diffusion coefficient D the only free fit parameters. The radius and length (ρ_0 and z_0, respectively) of the bleached spot were those measured from the three-dimensional confocal imaging of the spots described above.

Five different PVA films with different amounts of added glycerin were prepared. For each of these, several measurements of the recovery of the fluorescence in two-photon bleached spots were carried out, each giving a time series of fluorescence recovery such as shown in Figure 4. From these, values of the diffusion coefficient were determined using the procedure described in the previous section. The results of this analysis for all five samples are shown in Figure 5, giving the diffusion coefficient as a function of the amount of the plasticizer. There seems to be a very rough linear dependence of log D on the concentration of glycerin. A line fitted to these data is also shown in the figure. This trend is not likely to continue to higher values of glycerin concentration, since an extrapolation to 100% glycerin gives a value of $D \approx 4 \times 10^{-3}$ cm^2/s, far greater than the expected value. The value of D in pure glycerin can be estimated to be on the order of 10^{-9} cm^2/s, using the ratio of the viscosities of water and glycerin (~1000) and the reported values of the diffusion coefficient of Rhodamine 6G in water (2.8×10^{-6} cm^2/s).[32] With more data, a nonlinear fitting based on a model of diffusion in a plasticized polymer could yield valuable insight into molecular level diffusion processes.

The results at higher diffusion coefficients show significantly more fluctuations. This is mainly due to

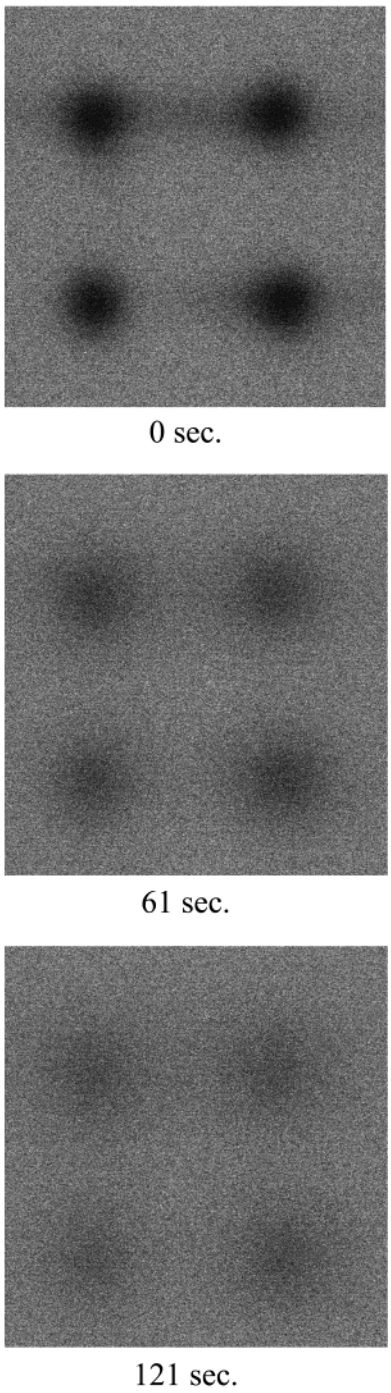

Figure 3. Time series of fluorescence of a spot bleached using two-photon absorption by Rhodamine B doped into a PVA/glycerin film.

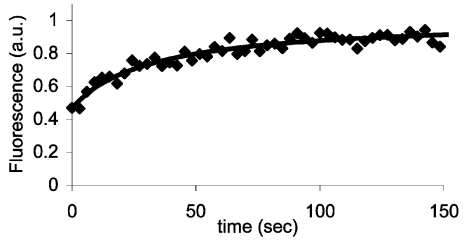

Figure 4. Time dependence of the fluorescence recovery in a PVA/glycerin film at the spot center. The line is a fit to the data of eq 6, yielding a value of $D = 3.2 \times 10^{-11}$ cm^2/s.

the error introduced by the inaccuracy in the determination of the exact time zero for the fluorescence recovery. Since the fluorescence recovery is more rapid, the precise value used for this time has more influence on the resulting fit parameters.

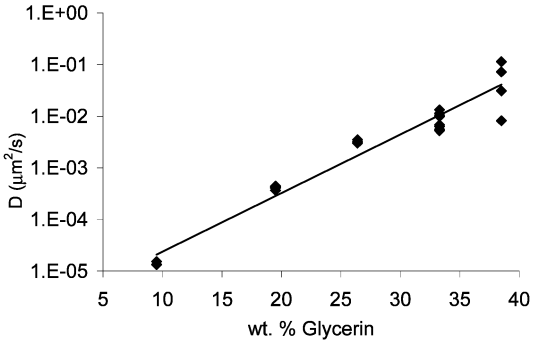

Figure 5. Diffusion coefficient vs amount of glycerin in a PVA matrix.

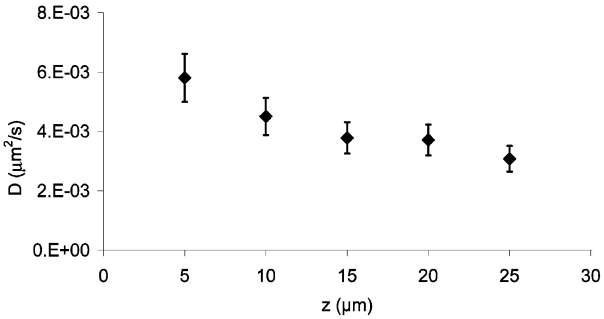

Figure 6. Diffusion coefficient of dye molecule vs depth from the film surface.

Three-Dimensional Mapping of Diffusion Coefficients. Besides the higher resolution, a great advantage of both confocal and two-photon microscopy is the ability to image in three dimensions. This advantage extends to the TP-FRAP technique, enabling a three-dimensional map of diffusion in an inhomogeneous sample to be generated and from that information about the sample morphology to be obtained.

We demonstrated this in a similar sample of PVA. A $\sim$30 μm thick film of PVA doped with Rhodamine B was prepared by doctor blading. After it had dried, a drop of glycerin was placed on top of the film and left overnight (15 h). The following day the glycerin was removed from the film surface. We conjectured that the glycerin slowly leaches into the polymer film, causing the creation of a concentration gradient vs depth. This would result in a gradient in the local viscosity and likewise in the diffusion coefficient of small molecules. The hypothesis was tested using 2P-FRAP to image the diffusion coefficient of the Rhodamine B as a function of distance from the film surface.

Bleached spots were created at five depths into the film. For each depth, a 2 $\times$ 2 array was bleached and imaged as a function of time after bleaching. Using the same procedure as described earlier, the recovery of the fluorescence in the bleached area was analyzed, yielding diffusion coefficients at each layer. The average diffusion coefficients as functions of depth into the film are shown in Figure 6. As expected, there was a drop in the diffusion coefficient going into the film, by a factor of about half over 20 μm. We surmised that near the film surface the larger concentration of glycerin plasticizer resulted in a higher diffusion coefficient. The monotonically decreasing diffusion coefficient suggested a similar decrease in glycerin concentration into the film depth.

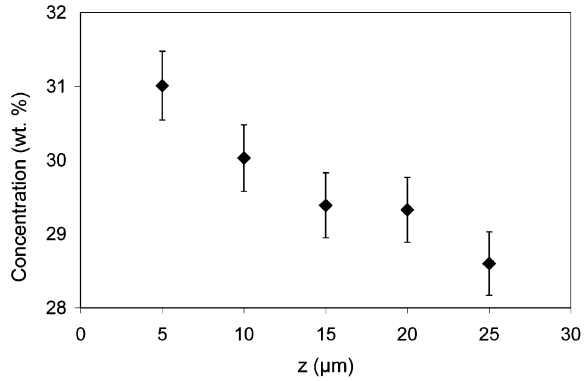

Figure 7. Estimate of glycerin concentration vs depth corresponding to the data in Figure 6, using the calibration from Figure 5.

As noted earlier, a large part of the error is due to uncertainty in the exact time-zero input into the fitting routine. This statistical uncertainty could be improved with more data.

This result was further quantified by estimating the local concentration of the glycerin from the measured diffusion coefficient. Using the relation between diffusion coefficient and glycerin concentration determined in the previous section (see Figure 5), we estimated the corresponding glycerin concentration as a function of depth. Figure 7 shows the results of this calculation. While the uncertainty in the results is significant, especially in this range of larger values of the diffusion coefficient, the clear drop of nearly half in the diffusion coefficient would correspond to a change of only 2.5 wt % in glycerin concentration according to Figure 5. More controlled experiments with thicker films are planned to confirm the effects presented here.

The effect of plasticizers on polymers has been characterized using techniques such as differential scanning calorimetry and mechanical properties;[31,33] however, these are bulk measurements. TP-FRAP enables the mapping of the plasticizer effects in inhomogeneous samples. In general, the uptake of fluids into polymer films is related to numerous industrial applications, either as an undesired effect or as a key property. The ability to map changes due to fluid absorption in three dimensions, and with micron spatial resolution, is a powerful tool for understanding polymer morphology changes at the microscopic level. For example, poly(vinyl alcohol) and related materials are commonly used for their water absorbent ability. Water absorption should result in a significant increase in the diffusion coefficient of fluorescent dyes doped into the film, and so 2P-FRAP could be used to quantify the absorption as a function of position or time. Another potential use is for characterizing water absorption into hydrophobic polymer coatings, which often are meant to prevent water penetration.[34] The ability of the FRAP technique to image slow diffusion processes makes it ideal for studying water penetration into these coatings, and the ability to measure gradients into the film using 2P-FRAP will enable optimization of thicknesses for specific film formulations.

Conclusion

We have demonstrated the determination of diffusion coefficients in polymer films using two-photon fluorescence recovery after photobleaching. Bleaching with two-photon excitation allowed a high spatial resolution and greater depth into the sample than standard single photon bleaching, and the simple ellipsoidal form of the bleached regions enabled a straightforward determination of the diffusion coefficients. Furthermore, the ability to bleach and image into the sample depth allowed us to measure the diffusion coefficient profile in three dimensions. We demonstrated the use of this technique by measuring a diffusion coefficient gradient caused by leaching of glycerin into a PVA film. Using a calibration correlating glycerin concentration with the diffusion coefficient, we were then able to determine a depth profile of the glycerin concentration.

References and Notes

(1) Muhr, A. H.; Blanshard, J. M. V. *Polymer* **1982**, *23*, 1012−1026.
(2) Berne, B.; Pecora, R. *Dynamic Light Scattering: With Applications to Chemistry, Biology, and Physics*; R.E. Krieger Pub. Co.: Malabar, FL, 1990. Chu, B. *Laser Light Scattering: Basic Principles and Practice*; Academic Press: Boston, 1991.
(3) Elson, E. L.; Magde, D. *Biopolymers* **1974**, *13*, 1−27.
(4) Thomson, N. L. In *Topics in Fluorescence Spectroscopy*; Lakowicz, J. R., Ed.; Plenum Press: New York, 1991; Vol. 1, pp 337−378.
(5) Schrof, W.; Klingler, J. F.; Rozouvan, S.; Horn, D. *Phys. Rev. E* **1998**, *57*, R2523−R2526.
(6) Kowert, B.; Dang, N.; Sobush, K.; Seele, L. *J. Phys. Chem. A* **2001**, *105*, 1232−1237.
(7) Duval, F. P.; Porion, P.; Van Damme, H. *J. Phys. Chem. B* **1999**, *103*, 5730−5735.
(8) Veniaminov, A.; Jahr, T.; Sillescu, H.; Bartsch, E. Length Scale Dependent Probe Diffusion in Drying Acrylate Latex Films. *Macromolecules* **2002**, *35*, 808−819.
(9) Peters, R.; Peters, J.; Tews, K. H.; Bähr, W. *Biochim. Biophys. Acta* **1974**, *367*, 282−294.
(10) Axelrod, D.; Koppel, D. E.; Schlesinger, J.; Elson, E.; Webb, W. *Biophys. J.* **1976**, *16*, 1055−1069.
(11) Jacobson, K.; Wu, E. S.; Poste, G. *Biochim. Biophys. Acta* **1976**, *433*, 215−222.
(12) Schlessinger, J.; Koppel, D. E.; Axelrod, D.; Jacobsen, K.; Webb, W. W.; Elson, E. L. *Proc. Natl. Acad. Sci. U.S.A.* **1976**, *73*, 2409−2413.
(13) Blonk, J. C. G.; Don, A.; Van Aalst, H.; Birmingham, J. J. *J. Microsc.* **1993**, *169*, 363−374.
(14) Peters, R.; Scholz, M. In *New Techniques of Optical Microscopy and Microspectroscopy*; Cherry, R. J., Ed.; CRC Press: Boca Raton, FL, 1991; pp 199−228.
(15) Smith, B. A.; McConnell, H. M. *Proc. Natl. Acad. Sci. U.S.A.* **1978**, *75*, 2759−2763.
(16) Bechhoefer, J.; Géminard, J.-C.; Bocquet, L.; Oswald, P. *Phys. Rev. Lett.* **1997**, *79*, 4922−4925.
(17) Wedekind, P.; Kubitscheck, U.; Peters, R. *J. Microsc.* **1994**, *176*, 23−33.
(18) Cutts, L. S.; Roberts, P. A.; Adler, J.; Davies, M. C.; Melia, C. D. *J. Microsc.* **1995**, *180*, 131−139.
(19) Kubitscheck, U.; Tschodrich-Rotter, M.; Wedekind, P.; Peters, R. *J. Microsc.* **1998**, *192*, 126−138.
(20) Gu, M.; Sheppard, C. J. R. *J. Microsc.* **1995**, *177*, 128−137.
(21) Brown, E. B.; Wu, E. S.; Zipfel, W.; Webb, W. W. *Biophys. J.* **1999**, *77*, 2837−2849.
(22) Williams, R. M.; Piston, D. W.; Webb, W. W. *FASEB J.* **1994**, *8*, 804−813.
(23) Centonze, V. E.; White, J. G. *Biophys. J.* **1998**, *75*, 2015−2024.
(24) Davis, S.; Bardeen, C. *Rev. Sci. Instrum.* **2002**, *73*, 2128−2135.
(25) Piston, D. W.; Wu, E. S.; Webb, W. W. *FASEB J.* **1992**, *6*, A34.
(26) Kubitscheck, U.; Tschodrich-Rotter, M.; Wedekind, P.; Peters, R. *J. Microsc.* **1996**, *182*, 225−233.
(27) Xu, C.; Webb, W. *J. Opt. Soc. Am. B* **1996**, *13*, 481−491.
(28) Wakebe, T.; Van Keuren, E. *Jpn. J. Appl. Phys.* **1999**, *38*, 3556−3561.
(29) Van Keuren, E.; Schrof, W. *Macromol. Rapid Commun.* **2002**, *23*, 1138−1140.

(30) Crank, J. *The Mathematics of Diffusion*, 2nd ed.; Clarendon Press: Oxford, 1975.
(31) Sakellariou, P.; Hassan, A.; Rowe, R. C. *Eur. Polym. J.* **1993**, *7*, 937−943.
(32) Rigler, R.; Mets, Ü.; Widengren, J.; Kask, P. *Eur. Biophys. J.* **1993**, *22*, 169−175.
(33) Sears, J. K.; Darby, J. R. *The Technology of Plasticizers*; John Wiley: New York, 1982.
(34) Browning, C. *Polym. Sci. Eng.* **1978**, *18*, 16−24.

MA034022S